

parental cells (Fig. 1, A and B). On comparative genomic hybridization arrays, the *EGFR* locus appeared further amplified in erlotinib-resistant (ER) and BIBW-2992-resistant (BR) cells compared to parental cells (fig. S1, A and B). Fluorescence in situ hybridization (FISH) analyses indicated that *EGFR* alleles were not amplified on double-minute chromosomes, as reported in other studies (21) (fig. S1C). The resistant cells had no evidence of *MET* amplification, another mechanism of acquired resistance to EGFR TKIs (fig. S1, A and B) (20, 22). No other obvious amplifications or deletions were found.

DNA from polyclonal PC-9/ER and PC-9/BR cells harbored the T790M allele plus the primary drug-sensitizing exon 19 del (Fig. 1C). No other mutations were found within any coding exons of *EGFR*. Analysis of cloned PC-9/BR complementary DNA (cDNA) products generated by reverse transcription-polymerase chain reaction (RT-PCR) showed that the T790M mutation was in cis with the primary drug-sensitive mutation. Signaling within the EGFR pathway was minimally affected by erlotinib in the PC-9/ER cells or by BIBW-2992 in the PC-9/BR cells (Fig. 2C and fig. S1D). Phospho-receptor tyrosine kinase arrays showed grossly similar profiles for PC-9/ER and PC-9/BR cells (fig. S1E).

Restoration of drug sensitivity after EGFR TKI withdrawal

We cultured resistant polyclonal cells in the absence of drug. After eight passages, PC-9/BR cells regained partial sensitivity to BIBW-2992 (Fig. 2A, upper panel). By 16 passages, drug sensitivity was restored to parental levels (Fig. 2A, lower panel). Loss of resistance corresponded with a decrease in the proportion of the T790M allele (Fig. 2B). Consistent with these data, lysates from parental cells and late-passage PC-9/BR-resistant cells treated with BIBW-2992 showed significantly reduced phosphorylation of EGFR and its downstream targets, extracellular signal-regulated kinase (ERK) and AKT, whereas lysates from resistant cells maintained in the presence of TKI and treated with the same concentrations of drug did not (Fig. 2C).

To extend our observations, we examined other *EGFR*-mutant isogenic pairs of drug-sensitive and drug-resistant lung cancer cell lines. Like PC-9 cells, HCC827/ER cells (19 del + T790M) regained TKI sensitivity after multiple passages in the absence of inhibitor and lost the T790M allele (fig. S2, A and B). By contrast, H3255 (L858R) cells, which also acquired T790M in response to continuous TKI exposure, neither regained TKI sensitivity nor lost the T790M after multiple passages in the absence of inhibitor, and they grew at the same rate as the parental line (fig. S3). Thus, two of three lines studied displayed resensitization. We characterized representative PC-9/BR cells in more detail.

Growth of parental cells and EGFR-mutant cells with T790M

To investigate the growth properties of drug-sensitive and drug-resistant cells, we counted the total number of viable cells in culture after plating each cell cohort in the absence of drug. To avoid contact inhibition as a confounding factor, cultures were not allowed to reach confluence. The parental cultures always had more cells (Fig. 2D) and showed more DNA synthesis (Fig. 2E) than did PC-9/BR cells. On average, parental cells doubled ~1.22 times faster than T790M-containing resistant cells. PC-9/BR cells withdrawn from drug for 25 passages (P-25) displayed parental growth kinetics (Fig. 2F). PC-9/ER cells harboring T790M followed the same slower growth pattern as PC-9/BR cells (fig. S2C).

To confirm these observations, we established single-cell clones from both PC-9/BR and PC-9/ER cell lines. Six T790M-containing clones

were derived in the presence of BIBW-2992 from the PC-9/BR cells. All clones displayed slower growth kinetics compared to parental cells or polyclonal resistant cells that had been passaged 25 times without drug. PC-9/BR clones also grew more slowly than the resistant polyclonal population maintained under selective pressure (Fig. 2F). Four T790M-harboring clones were derived in the presence of erlotinib from PC-9/ER cells and showed analogous characteristics (fig. S2, D and F). The growth properties of parental cells and PC-9/BR-resistant clones were also maintained in vivo (Fig. 2G). We saw no differences in cell cycle profiles, rates of apoptosis, or rates of senescence between parental and resistant cells. Notably, the T790M-harboring cells described here are distinct from the recently described subpopulation of *EGFR*-mutant cancer cells lacking T790M that transiently exhibit a distinct phenotype characterized by the engagement of insulin-like growth factor 1 receptor (IGF-1R) activity, hypersensitivity to histone deacetylase (HDAC) inhibition, altered chromatin, and an intrinsic ability to tolerate drug exposure (23).

Collectively, these results can be explained by two scenarios (Fig. 2H). First, tumor cell populations with acquired resistance are composed of a heterogeneous mixture of cells, some of which harbor the T790M allele. After drug withdrawal, previously growth-arrested but faster-growing TKI-sensitive cells repopulate the tumor, and the population of cells displays resensitization. In the second possibility, tumor cell populations with acquired resistance are composed of a homogeneous group of resistant cells; after drug withdrawal, every cell loses the T790M allele and the population becomes resensitized. Several lines of evidence support the former possibility. Polyclonal populations of resistant cells "lose" the T790M allele after passages in vitro in the absence of inhibitor. By contrast, single-cell clones harboring T790M retain the allele even after multiple passages in the absence of drug in vitro (fig. S2, E and F) and as xenografts (up to 78 days) (Fig. 2G and fig. S2G). Retention of the T790M allele in the single-cell clones, both in vitro and in vivo, suggests that acquisition of that allele is not reversible within individual cells, making the second scenario less likely.

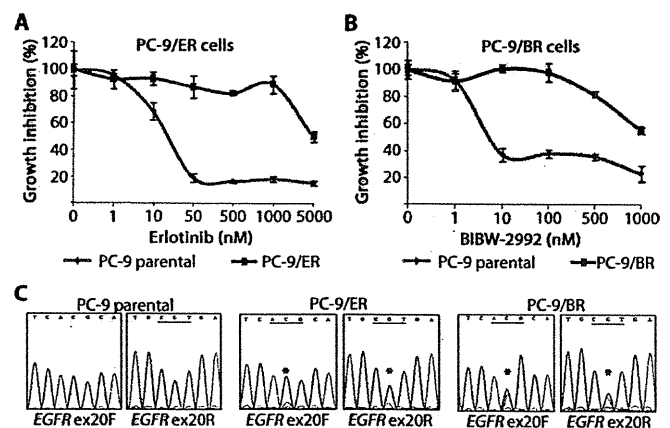


Fig. 1. Derivation and characterization of TKI-resistant cells. (A and B) PC-9 erlotinib-resistant cells (PC-9/ER) (panel A) and PC-9 BIBW-2992-resistant cells (PC-9/BR) (panel B) were derived after ~120 days of culture with increasing concentrations of drug. Growth inhibition assays show that these cells are resistant to respective TKIs compared to the parental cells. (C) Direct dideoxynucleotide sequencing chromatograms from *EGFR* exon 20 (ex20) show the presence of the T790M mutation (*ACG→ATG) in the PC-9/ER and PC-9/BR cells but not in parental cells. F, forward; R, reverse directions.

Effect of the percentage of T790M clones on the sensitivity and growth of a population of mixed tumor cells

Biopsies of growing lesions in patients do not provide information on whether a tumor consists of a heterogeneous mix of sensitive and resistant cells or a homogeneous mass of only resistant cells (Fig. 2H),

because which cells harbor the T790M mutation cannot be ascertained directly. To estimate the proportion of T790M-containing cells within a population necessary for the entire population to display resistance, we performed reconstitution experiments. T790M-harboring clonal cells (PC-9/BR clone 1) were mixed with TKI-sensitive parental cells

at known percentages (Fig. 3A), and cell mixture drug sensitivity was measured by growth inhibition assays. Populations with small percentages of resistant cells (1 and 10%) displayed similar sensitivity to erlotinib as parental cells (0%), whereas sensitivity was reduced when T790M clones made up >25% of the population (Fig. 3B). These data can explain why patients whose tumors harbor low levels of T790M can still undergo an objective radiographic response to EGFR TKI treatment (24, 25).

We next estimated the percent of resistant cells needed in a population of cells to display tumor growth. Cell mixtures were treated with dimethyl sulfoxide (DMSO) or 1 μ M erlotinib for 72 hours (Fig. 3C). The addition of erlotinib did not alter the growth of cell populations with low proportions of resistant cells (1%). However, compared to DMSO-treated cells, populations containing greater than 10% T790M-positive cells proliferated faster than parental cells (0%) in the presence of drug. These findings are further consistent with the notion that tumor cell populations with acquired resistance to EGFR TKIs can be composed of heterogeneous tumor cell mixtures.

Biological properties of sensitive and resistant cells compared to EGFR-mutant NSCLC in human patients

The T790M substitution confers synergistic kinase activity and transformation potential when combined with drug-sensitive EGFR mutations (5, 14). We had therefore expected that resistant clones harboring the T790M allele would display a growth advantage compared to parental drug-sensitive cells. Our results to the contrary prompted us to examine the clinical course of patients with EGFR-mutant NSCLC to verify that our preclinical findings reflected the human disease.

First, we asked what percentage of patients with EGFR-mutant tumors could remain on long-term EGFR TKI therapy. We analyzed unpublished data from patients enrolled in NEJ002, a prospective trial for patients with untreated metastatic

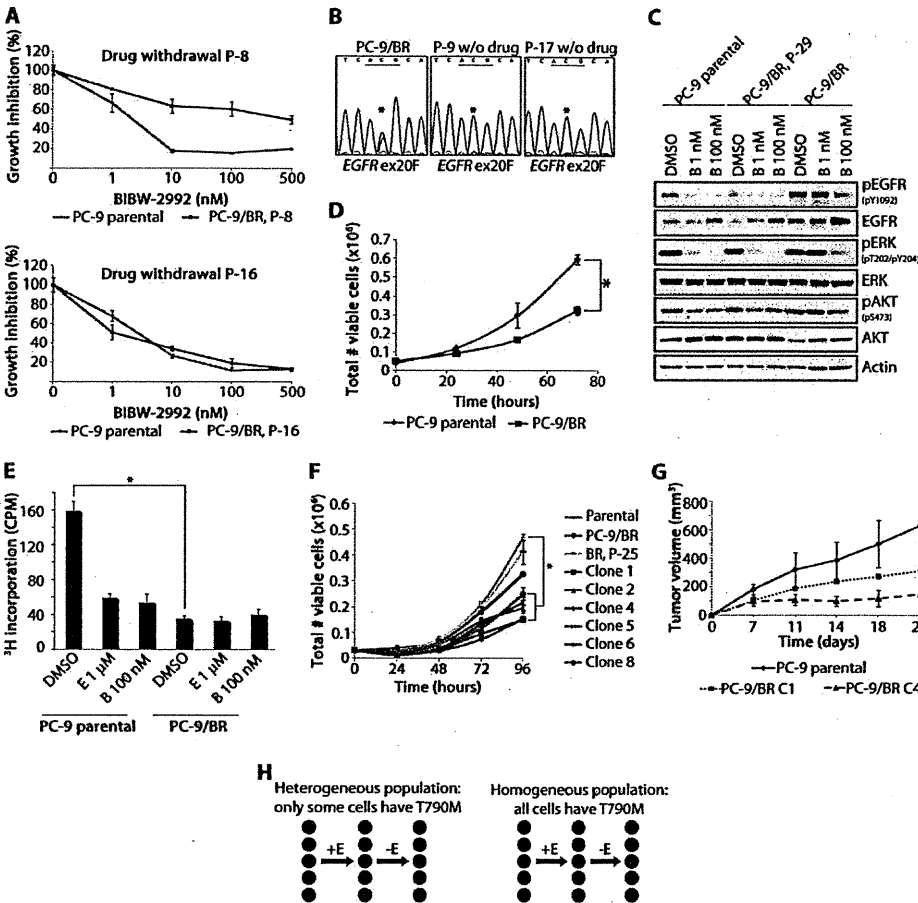


Fig. 2. Growth characteristics of TKI-sensitive and TKI-resistant cells. (A) Polyclonal PC-9/BR cells cultured without BIBW-2992 for 8 and 16 passages (P-8 and P-16, respectively) regained intermediate and complete sensitivity to BIBW-2992, respectively. (B) Sequencing of EGFR exon 20 (ex20) showed a decrease in the T790M allele that correlates with restored TKI sensitivity. Genomic DNA was extracted from cells after 9 and 17 passages (P-9 and P-17, respectively) without drug (*ACG→ATG). (C) Parental and late-passage resistant cells (P-29) show decreased phosphorylation of EGFR and its downstream targets in the presence of BIBW-2992, whereas signaling in the PC-9/BR cells remained intact. Cells were treated with vehicle (DMSO) or BIBW-2992 (B) for 3 hours. (D) T790M-containing PC-9/BR cells proliferated more slowly than parental cells over 72 hours in the absence of inhibitor. Graphs represent the average of triplicate wells \pm SD. * $P < 0.01$. (E) [3 H]Thymidine incorporation confirms the slower proliferation rate of the PC-9/BR cells compared to parental cells. Cells were treated with DMSO, erlotinib (E), or BIBW-2992 (B) for 24 hours. Data are expressed as counts per million (CPM) relative to each other. (F) Cell counts for PC-9 parental cells, BR (polyclonal), BR late-passage (P-25), and T790M-containing BR clones (1, 2, 4, 5, 6, 8) show that the clones grow more slowly than parental and P-25 cells. (G) PC-9 parental and PC-9/BR cells (clones 1 and 4) were injected subcutaneously into nude mice, and tumor growth in the absence of drug was monitored over time. The slower growth pattern of T790M-harboring PC-9/BR clones 1 and 4 is maintained in vivo. Data are average tumor volumes ($n = 3$ per group) \pm SEM. (H) At the onset of acquired resistance, an EGFR-mutant tumor (blue) develops T790M in a small proportion of cells (red) after exposure to erlotinib (E; left). Upon withdrawal of drug, previously growth-arrested TKI-sensitive cells repopulate the tumor. Alternatively (right), all cells contain some level of T790M at progression. Upon discontinuation of the inhibitor, all cells revert back to parental genotype.

EGFR-mutant tumors (7), to evaluate the range of time on TKI therapy. Although the median duration on gefitinib was 0.83 years, the range was as high as 3.3 years (Fig. 4A). Patients (32, 4, and 1%) were on drug for 1, 2, and 3 years, respectively. These data are consistent with the notion that some EGFR-mutant tumors display indolent progression.

Second, we examined the prospective clinical course of patients with EGFR-mutant tumors and T790M-mediated acquired resistance. We extracted unpublished data from a clinical trial in which a cohort of 14 patients was treated prospectively with erlotinib (26). There were four patients whose tumors had a documented T790M mutation at the time of disease progression, two of whom had measurable disease amenable to analysis. Both patients displayed slow growth of the T790M-harboring lesion (Fig. 4, B and C, and fig. S4). In the first case, the patient was biopsied when she was deemed to have progression of disease after 25 months (11). Analysis of previous computed tomography (CT) scans indicated that the tumor began to grow at least 6 months before the biopsy and that it grew slowly from the time of maximal response (Fig. 4C). The second patient showed similar findings (fig. S4A). By comparison, a similar analysis of two patients with EGFR wild-type tumors that progressed after receiving benefit from first-line chemotherapy (27) showed that both displayed rapid tumor growth from the time of maximal response to the time when criteria for progressive disease were met (fig. S4B). Notably, the median time to progression on chemotherapy is ~4 months in unselected NSCLC but more than 9 months on erlotinib for EGFR-mutant tumors (10, 28).

Third, using unpublished data from the same prospective erlotinib study that was used for image analysis (26), we asked what proportion of patients displayed progression of disease on erlotinib but continued a TKI as a result of indolent tumor growth (Fig. 4, B and C, and fig. S4A). Among 14 patients, 4 patients continued on single-agent TKI for at least 6 months beyond disease progression, because they were relatively asymptomatic (Fig. 4D). Three of the four patients had biopsies within

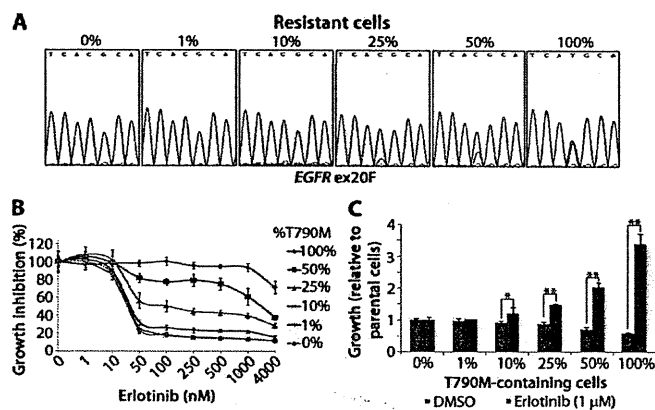


Fig. 3. Reconstitution experiments to study T790M-mediated resistance. (A) T790M-containing PC-9 cells (BR, clone 1) were spiked into parental PC-9 cells at various proportions. The increased proportion of the T790M allele (*ACG→ATG) is evident from representative direct sequencing chromatograms of EGFR exon 20. (B) Mixed populations of cells were treated with increasing concentrations of erlotinib for 72 hours, at which point growth inhibition was measured. (C) Cell populations with varying proportions of T790M-containing cells were grown in the presence of DMSO or erlotinib (1 μM) to mimic various states of a TKI-resistant heterogeneous solid tumor. Total cell number was determined after 72 hours and graphed as the percent growth compared to parental cells (0%) ± SD. **P* < 0.05; ***P* < 0.01.

2 months of coming off study, and all three (patients B, C, and D) harbored the T790M mutation. T790M was also detected in the re-biopsy specimen from one patient despite the addition of chemotherapy to continuous erlotinib treatment.

Fourth, we examined the frequency of the T790M allele by using 454 sequencing of DNA extracted from 16 untreated early-stage resected EGFR-mutant NSCLCs (Table 1). From mutant allele dilution experiments, the limit of detection of the 454 method was ~0.2%. We did not detect the T790M allele in any of the resected specimens or in parental PC-9 cell DNA. These data are consistent with our evolutionary modeling results (see below) and demonstrate that in the absence of TKI selection, the T790M allele is either absent or highly infrequent (less than 1 in 500).

Finally, numerous published reports support our preclinical data: (i) EGFR-mutant tumors can “flare” after patients stop EGFR TKI treatment (29); (ii) serial biopsies over the course of treatment demonstrate a decrease in prevalence of the T790M allele during the period off therapy (30); (iii) EGFR-mutant cancers that recur after stopping adjuvant TKI do not harbor the T790M mutation, suggesting a growth disadvantage to these clones (31); (iv) EGFR-mutant tumors with documented progression can re-respond to an EGFR TKI after a hiatus off TKI therapy (30, 31); (v) patients with EGFR-mutant tumors and T790M-mediated acquired resistance paradoxically have a better survival than those with acquired resistance and no T790M (32, 33); and (vi) ultra-sensitive locked nucleic acid technology (LNA-PCR; limit of detection ~0.1%) was unable to detect T790M in TKI-naïve samples, half of which harbored the mutation upon progression (33). Collectively, these data

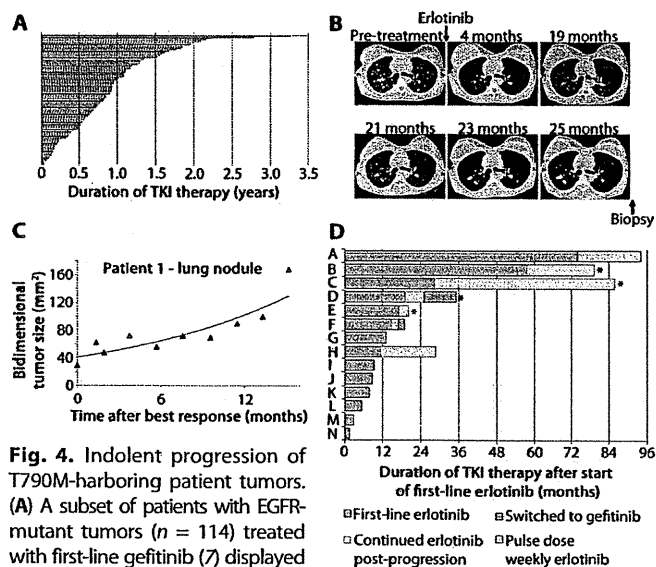


Fig. 4. Indolent progression of T790M-harboring patient tumors. (A) A subset of patients with EGFR-mutant tumors (*n* = 114) treated with first-line gefitinib (7) displayed prolonged responses to treatment. The average time on gefitinib before progression was 0.9 years. (B) Serial computed tomography scans from a patient with an EGFR-mutant tumor (ex 19 del) [images from (11)]. (C) Serial bidimensional measurements taken from the time of best response for the patient in panel B illustrate the slow rate of progression in this lesion. (D) Patients receiving first-line erlotinib as part of a phase II trial. Four of 14 patients (28%; patients B, C, D, and H) were continued on treatment with single-agent TKI (erlotinib or gefitinib) for >6 months after RECIST progression. Asterisk denotes the presence of T790M.

Downloaded from stm.sciencemag.org on August 6, 2011

all support the notion that tumors with acquired resistance to gefitinib or erlotinib may be composed of mixed populations of cells, and continued TKI selection is needed to promote the outgrowth of slower-growing T790M-mutant cells.

Evolutionary cancer modeling applied to EGFR-mutant NSCLC

Having established the clinical relevance of our preclinical models, we applied evolutionary cancer modeling, involving detailed mathematical descriptions of our tumor cell populations in vitro, to design optimized dosing strategies for EGFR-mutant NSCLC. We incorporated pharmacokinetic data from human clinical trials with erlotinib to ensure that the drug doses proposed were clinically achievable in humans (34, 35).

First, we tested whether this approach could be used to determine the potential frequency of T790M-containing clones within a population of untreated PC-9 cells. We measured the growth and death rates of PC-9 and PC-9/ER cells (see Materials and Methods) cultured in the presence of various doses of erlotinib (fig. S5) and modeled the drug-sensitive and drug-resistant cell populations as a multitype binary branching process (36). Application of the experimentally determined estimates of viable cells as well as apoptosis in the presence and absence of drug generated fitted curves describing the birth and death rates of both cell populations as a function of the concentration of erlotinib (Fig. 5, A to D). These curves were used to estimate the number of resistant cells

Table 1. 454 sequencing of EGFR exon 20. About 100,000 454 reads per sample were generated from PCR products generated with EGFR exon 20 (ex20)-spanning primers. All tumors were from treatment-naïve patients. TKI-R-1 and TKI-R-2 were run as positive control samples. 1^mmutn, primary EGFR mutation, as assessed by direct sequencing.

Sample	Stage	1 ^m mutn	454 ex20 T790M (%)
Lung TKI-R-1	IV	19 DEL	Y (59%)
Lung TKI-R-2	IV	L858R	Y (1.07%)
H3255	Cell Line	L858R	N
PC-9	Cell Line	19 DEL	N
130T	IA	19 DEL	N
169T	IA	19 DEL	N
230T	IA	19 DEL	N
474T	IA	19 DEL	N
631T	IA	19 DEL	N
20T	IB	19 DEL	N
734T	IB	19 DEL	N
739T	IB	19 DEL	N
388T	IIIA	19 DEL	N
3T	IA	L858R	N
5T	IA	L858R	N
485T	IA	L858R	N
570T	IB	L858R	N
685T	IB	L858R	N
25T	IB	L858R	N
166T	IB	L858R	N

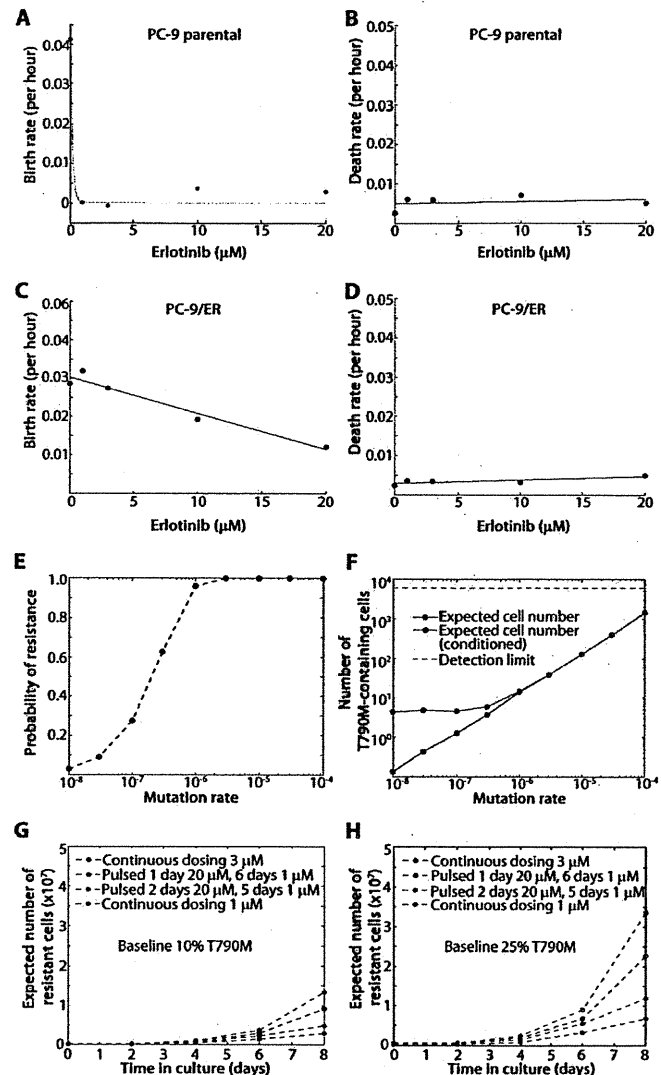


Fig. 5. Evolutionary cancer modeling predictions to delay the development of resistance. (A) PC-9 cell birth rate at erlotinib concentrations of 0, 1, 3, 10, and 20 μ M. (B) PC-9 cell death rate as a function of increasing erlotinib concentration. (C) PC-9/ER cell birth rate in the presence of erlotinib (0, 1, 3, 10, and 20 μ M). (D) PC-9/ER cell death rates as a function of increasing erlotinib concentration. (E) Probability of preexisting T790M-harboring cells in a population of 3 million cells initiating from one cell harboring just a drug-sensitive EGFR mutation that grew in the absence of drug for a range of mutation rates (10^{-4} to 10^{-8} per cell division). (F) Expected number of resistant cells present in the population, both averaged over all cases and averaged only over the subset of cases, where at least one resistant cell is present. (G) An initial population of 750,000 cells, 10% of which harbor T790M, treated with continuous low-dose erlotinib (1 and 3 μ M) selects for the emergence of T790M-harboring cells (green and black lines). The addition of one or two high-dose erlotinib "pulses" (20 μ M) followed by 1 μ M for the remaining days of a 7-day cycle decreases the expected number of resistant cells (red and blue lines). (H) Analogous results as in panel (G) starting with an initial population with 25% T790M-harboring cells.

Downloaded from stm.sciencemag.org on August 8, 2011

present in a population of 3 million cells [an estimate of the number of cells in a ~1-cm tumor (37)] that initiated from a single cell harboring only a drug-sensitive EGFR mutation and that grew in the absence of drug. The probability that at least one resistant cell exists in the 3 million cell population (Fig. 5E) ranged from 3% (for a mutation rate of 10^{-8} per TKI-sensitive cell division) to 100% (for mutation rates above 10^{-6}). We also estimated the number of T790M-containing cells expected when the population reaches 3 million cells for a range of mutation rates (10^{-4} to 10^{-8}) (Fig. 5F); we determined the expected number of cells both averaged over all cases and averaged over the subset of cases in which at least one resistant cell was present. By the standard estimate of mutation rates per base pair per cell division (10^{-8} to 10^{-7}) (38, 39), cells with T790M in the final population would be about 1 cell out of 3 million. These data were consistent with our 454 deep sequencing results (Table 1), which showed that T790M was rare (<0.2%) in untreated early-stage EGFR-mutant tumors.

Second, we used mathematical modeling to predict how long it would take to restore drug sensitivity in the PC-9/BR polyclonal resistant cell population, based on our cell growth and death rates. Using the observed doubling times for sensitive cells and resistant cells of ~19 hours and ~23 to 25 hours, respectively, we estimated that after drug withdrawal, about 35 to 40 days would be needed for a population of cells with 87.5% resistant cells to have only 1% resistant cells. These data fit well with the observation that between 8 and 16 passages (with 1 passage every 3 days) were required to restore full sensitivity after drug withdrawal (Fig. 2). Collectively, these data demonstrate that evolutionary cancer modeling could accurately describe and predict our biologically observed phenomena and were consistent with the presence of a mixed cell population in resistant tumors (Fig. 2H).

Modeling-predicted delay of resistance by high-dose pulses combined with a continuous low dose of TKI

We then used mathematical modeling to predict the relative effects of alternative dosing schedules on the development of resistance. Under the previously mentioned pharmacokinetic constraints, we hypothesized that intermittent high-dose pulses of erlotinib (20 μ M) in conjunction with a continuous low-dose administration (1 μ M) could be a tolerated dosing schedule to delay the establishment of large resistant cell populations. Using the cell growth and death rates calculated in the presence of 1 and 20 μ M erlotinib, we determined the number of PC-9/ER cells expected under various pulsed continuous treatment schedules, starting from an initial population of 750,000 cells with 10 and 25% of the population initially containing T790M (Fig. 5C). Modeling predicted that the use of continuous low-dose treatment with simultaneous high-dose pulsed administration of erlotinib should delay the acquisition of T790M-mediated resistance (Fig. 5, G and H).

To corroborate the mathematical predictions, we applied the calculated dosing schedules to our cell lines. Using T790M-harboring clones mixed with parental cells, we treated cell populations with 0, 25, or 100% resistant cells with erlotinib at the indicated doses for 7 days (one cycle, as modeled in Fig. 5H). As expected, T790M mutations were not selected for in the absence of drug in the population with 25% resistant cells but were enriched for when 1 μ M erlotinib was administered daily (Fig. 6A). Addition of one or two high-dose pulses of erlotinib (20 μ M) together with daily low-dose erlotinib (1 μ M) also selected for T790M-harboring cells in the mixed population. However, the frequency of the mutant allele was lower than

with daily dosing (Fig. 6A), consistent with our mathematical predictions (Fig. 5G) and with the notion that this regimen could delay the acquisition of T790M-mediated resistance.

To circumvent the limitations of erlotinib dosing (maximum of 20 μ M) and to apply our predictions to a long-term model, we substituted BIBW-2992, which is more potent against the T790M mutant, with an IC_{50} of about 100 nM (15). This concentration of drug can be achieved in humans at the standard dose of 40 mg daily (40). We used the same continuous dose escalation protocol as we used for erlotinib and BIBW-2992 to select for T790M-mediated resistance in PC-9 cells. Whereas T790M was detectable with low concentrations of BIBW-2992 and erlotinib alone, the combination of high-dose weekly BIBW-2992 plus continuous erlotinib did not select for this mode of resistance

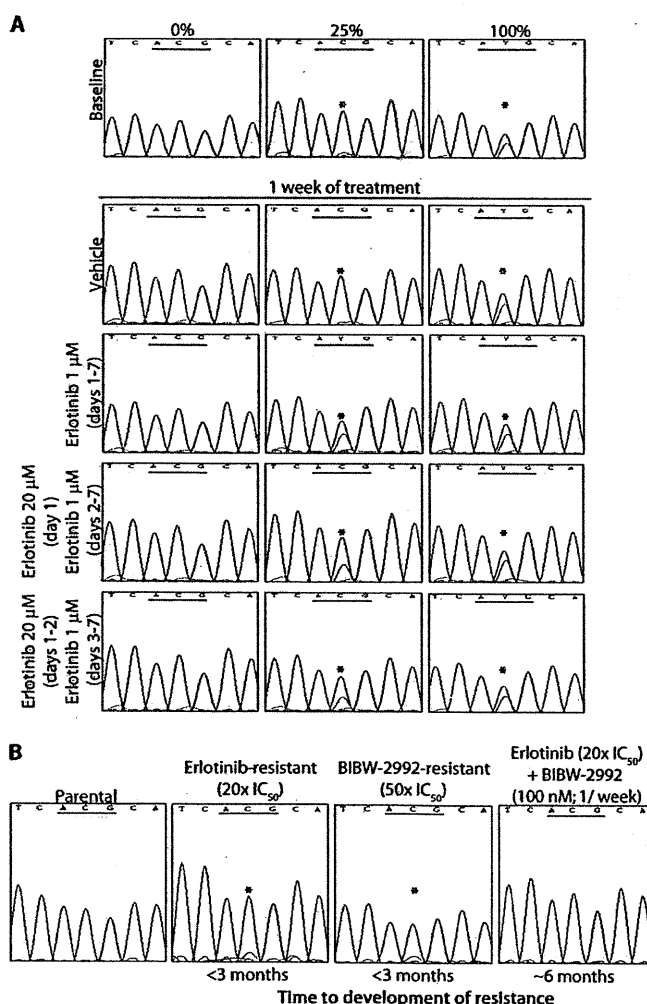


Fig. 6. Effect of pulsed high-dose TKI treatment on the number of T790M-harboring cells. (A) Using a T790M-harboring clone (PC-9/BR, c1), we mixed cell populations to have 0, 25, or 100% resistant cells. The baseline panel shows forward sequence tracings from exon 20 of EGFR (the underlined codon encodes T790). Cell populations were then treated with erlotinib at the indicated doses for 7 days. (B) Chromatograms display exon 20 forward sequences of EGFR from PC-9 cells treated with different drugs (*ACG→ATG).

Downloaded from stm.sciencemag.org on August 8, 2011

(Fig. 6B). Furthermore, the total time for the development of complete resistance (100- to 1000-fold the initial IC_{50}) was twice as long for cells treated with the pulsed dosing regimen. The mechanism of resistance in these cells remains under investigation. These data confirm the modeling predictions and show that resistance can be delayed with combination of a pulsed high-dose potent TKI and continuous low doses of erlotinib.

Modeling-predicted tumor cell control after the emergence of EGFR T790M by continuation of TKI therapy

We next used our models to predict better treatment strategies for patients whose tumor cell populations have developed T790M-mediated resistance. In standard oncology practice, progression while on a specific therapy leads to cessation of that therapy and initiation of a new treatment. However, our data suggest that resistant tumors may be composed of a heterogeneous mix of TKI-sensitive and TKI-resistant cells (Fig. 3) and that stopping TKI therapy may permit expansion of the faster-growing TKI-sensitive cells. We modeled this scenario in vitro by diluting PC-9 T790M-containing clonal cells in parental cells at various concentrations, as described above. Cell populations were treated with physiologically achievable doses of chemotherapy alone or chemotherapy plus erlotinib, and cell numbers were counted every 48 hours (Fig. 7A). We used two chemotherapeutic agents with activity in lung cancer: a platinum-based drug, cisplatin (41), and an antifolate, pralatrexate (42). The latter was used rather than the chemically related pemetrexed, because pralatrexate is more stable after reconstitution.

Cells treated with cisplatin (500 nM) (28) grew slower in the presence of erlotinib, both in vitro and in vivo (Fig. 7, B and C). Similar in vitro results were obtained with pralatrexate (100 μ M) (43) (fig. S6). Collectively, these data suggest that patients may benefit from continued

treatment with an EGFR TKI, even after developing T790M-mediated progression of disease.

DISCUSSION

All patients with metastatic EGFR mutant-harboring lung adenocarcinomas will eventually develop acquired resistance if treated with the EGFR TKIs gefitinib and erlotinib. In ~50% of cases, tumor cells harbor a second mutation in the EGFR kinase domain (T790M), which alters a gatekeeper residue within the ATP-binding pocket. Because existing treatment schedules were established empirically with drugs developed against wild-type EGFR, we hypothesized that evolutionary cancer modeling could be used to develop more optimal dosing strategies against the mutant receptors in NSCLC. We combined in vitro cell culture experiments, multiple clinically relevant data sets, and mathematical modeling to describe tumor behavior. We then used the models to predict dosing strategies that were validated in vitro and in vivo. These dosing regimens will need to be further validated in clinical trials with patients with EGFR-mutant lung cancer. We propose the use of high-dose pulsed once-weekly BIBW-2992 with daily low-dose erlotinib to delay the emergence of T790M-mediated resistance. PC-9 cells treated with this regimen required twice as long to develop resistance and did not show selection for T790M mutations. In patients, the combination of two EGFR TKIs could lead to overlapping toxicities involving rash and diarrhea. Thus, in a phase IB dose-safety trial, we would recommend a more tolerable strategy, with lower doses of erlotinib still known to be effective against EGFR-mutant tumors (25 or 50 mg daily, orally) (44). For BIBW-2992, we would suggest starting at 40 mg once a week and escalating to the maximum tolerated dose, aiming to achieve as high a concentration of the drug in patients as possible.

We determined that tumors with acquired resistance likely harbor mixed populations of drug-sensitive and drug-resistant cells with differential growth rates. To treat these tumors, we would propose continuing EGFR TKI suppression with chemotherapy beyond T790M-mediated progression for maximal disease control, based on the benefits of this approach in both in vitro and in vivo models. Such practice would be analogous to what is done for HER2-positive breast cancer patients who continue receiving the anti-HER2 antibody trastuzumab even after the development of progressive disease (45).

Our findings raise a paradox involving the T790M mutation. Surrogate kinase assays in Sf9 transfectants and transformation assays in fibroblasts showed that the addition of the T790M mutant to a drug-sensitive mutant confers synergistic oncogenic activity (5, 46). Yet, our preclinical data demonstrate that acquisition of the T790M mutation is associated with a growth disadvantage in the absence of TKI selection. One explanation is that the oncogenic activity of double-mutant EGFRs can be toxic to lung adenocarcinoma cells when the protein is expressed at a certain level. This hypothesis is supported by our own observations that transfectants with lower levels of the double-mutant receptor are spontaneously selected for over time (fig. S7A). Other lung cancer cells expressing a different gatekeeper mutation also display a growth disadvantage (fig. S7B). How double-mutant EGFR signaling leads to slower growth rates remains an area of investigation.

Although our preclinical data are supported by many data sets of patients with resectable early-stage to metastatic late-stage EGFR-mutant tumors, the slower growth rate of T790M-harboring cells in

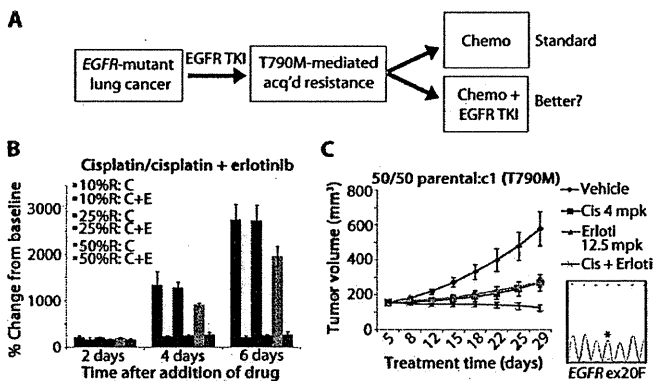


Fig. 7. Effect of continuation of TKI therapy with chemotherapy on heterogeneous TKI-resistant tumors. (A) Schematic outline of treatment options for patients with EGFR-mutant disease. (B) PC-9/BR c1-resistant cells were diluted in parental cells at various concentrations (see Fig. 3) and treated with chemotherapy (cisplatin, 500 nM) or chemotherapy plus erlotinib (3 μ M). In all cases, the TKI-chemotherapy combination was more efficacious at inhibiting cell growth. (C) Athymic nude mice with established tumors (50:50 mixture of PC-9 parental and BR c1 cells) were administered vehicle, cisplatin (4 mg/kg), erlotinib (12.5 mg/kg), or cisplatin plus erlotinib. At the start of treatment, T790M-containing cells made up ~25% of the population, as measured by direct sequencing (bottom right). Tumor volumes were graphed as averages ($n = 5$ per group) \pm SEM. mpk, mg/kg. * indicates residue of interest.

our *in vitro* models may not be representative of all T790M-positive cells in human patients. Consistent with this, one of the three isogenic pairs of EGFR drug-sensitive/drug-resistant cell lines that we developed did not display resensitization after drug withdrawal. Other factors, such as fibroblast growth factor receptor (FGFR), IGF-1R, and nuclear factor κ B (NF κ B) signaling, may also modulate responses to EGFR TKIs (47–49).

The characteristics of T790M-harboring NSCLC may be broadly applicable to other tumor types. For example, in gastrointestinal stromal tumors (GISTs) harboring imatinib-sensitive activating mutations in KIT, “flares” have been observed after imatinib cessation upon progression (50), and a recent clinical study showed that patients with documented imatinib resistance can re-respond to imatinib after a period off TKI therapy (51). Furthermore, an analogous *ABL* gatekeeper mutation (T315I) observed in imatinib-resistant chronic myelogenous leukemia (CML) cells decreases in abundance after imatinib therapy is stopped (52).

We predict that in patients with acquired resistance whose disease begins to accelerate rapidly, genetic alterations other than just the presence of the EGFR T790M mutation may play a role in tumor progression. That is, a third hit could enable escape from a slower growth phenotype and contribute to accelerated disease progression. Candidate third-hit genetic alterations remain to be identified.

In summary, evolutionary cancer modeling coupled with an understanding of the unique biological properties of TKI-sensitive and TKI-resistant cells has allowed us to propose optimized dosing schedules for the treatment of EGFR-mutant lung cancer. This approach could be more generally applied toward the optimization of dosing strategies of other targeted therapies used against oncogene-driven cancers.

MATERIALS AND METHODS

Patient samples and data

Tumor specimens were obtained with patients’ consent under Memorial Sloan-Kettering Cancer Center (MSKCC) Institutional Review Board–approved protocols. Samples were frozen and stored at -80°C in institutional tumor banks.

CT scans from four patients treated prospectively with erlotinib (26) who then developed T790M-containing tumors were available for analysis (11). Two patients had a complete response with no residual measurable disease, leaving two patients evaluable. The presence of T790M was confirmed in rebiopsy samples from the remaining two patients after progression of disease, as determined by Response Evaluation Criteria in Solid Tumors (RECIST) (53). These cases were re-reviewed for characteristics of indolent progression. Serial bidimensional measurements of reference lesions were performed by a radiologist (M.S.G.) from the time of best response.

Growth assays

Growth inhibition was measured with CellTiter Blue Reagent (Promega) as per the manufacturer’s instructions using cells plated in triplicate at a density of 4000 cells per well. Fluorescence was measured on a SpectraMax fluorometer. Growth inhibition was calculated as percentage of vehicle-treated wells \pm SD.

For PC-9 cell counting assays, 20,000 to 40,000 cells per well were plated in six-well plates. Cell counting was performed in triplicate with an automated ViCell counter (Beckman Coulter) or a Coulter Counter.

H322M cells were plated at a density of 100,000 per well and counted in quadruplicate with a Z2 Coulter Counter (Beckman Coulter). Cells were not allowed to reach $>70\%$ confluence at the final time point. Statistical significance was determined with the Student’s two-tailed *t* test. For all assays conducted in the presence of drug, fresh TKI was added every 72 hours.

For reconstitution experiments, PC-9/BR C1 cells were mixed with parental cells at the indicated concentrations before plating. DNA was isolated in parallel from each dilution for PCR-based EGFR exon 20 sequencing to confirm mutant peak levels. All experiments were conducted at least two independent times.

Mathematical modeling

PC-9 and PC-9/ER populations were modeled as a two-type stochastic birth and death process. In the context of our model, each PC-9 or PC-9/ER cell waits an exponentially distributed amount of time to divide or die; this waiting time is governed by the cell birth and death rates. During PC-9 cell replication, a cell harboring the T790M mutation arises with a given probability (the mutation rate). Sensitive and resistant cells have distinct growth and death rates that vary depending on the drug concentration; these parameters were experimentally determined. We estimated the net (birth minus death) growth rate by fitting the mathematical model to cell counts at 48, 60, and 72 hours in the presence and absence of drug. Death rates were estimated from annexin V/propidium iodide fluorescence-activated cell sorting (FACS) counts; we considered double-positive cells to make up the dead cell population. We accounted for cell clearance by assuming that 50% of dead cells are cleared every 12 hours; this assumption was made to account for the degradation of dead cells in the cell culture over time. Measurements were performed at drug concentrations of 0, 1, 3, 10, and 20 μM erlotinib (Fig. 5A).

To calculate the expected frequency of T790M alleles in a population of 3 million cells that initiated with a single cell harboring only a drug-sensitive EGFR mutation and growing in the absence of drug, we used the growth and death rates obtained in the absence of drug (0 μM data point). We performed 100,000 Monte Carlo simulations of the model ending when the total population reaches the desired size (3 million cells). We recorded the number of resistant cells present at the final time point. For details, see (18, 54).

To compare the relative effects of various dosing strategies on the development of resistance, we used analytical formulas describing the expected resistant cell population size under time-dependent dosing strategies. These calculations are based on the generating function for an inhomogeneous two-type birth and death process; birth and death rates of the sensitive and resistant cell population at each drug concentration are informed by data shown in Fig. 5A [see (18, 55)].

Xenograft studies

Cells (5×10^6 to 10×10^6) were injected with Matrigel into the hind flanks of 8-week-old athymic (*nu/nu*) female mice (Harlan). When tumors reached $\sim 150 \text{ mm}^3$, animals were randomized to receive vehicle alone, cisplatin (4 mg/kg twice per week, intraperitoneally), erlotinib (12.5 mg/kg daily, orally), or a combination of both erlotinib and cisplatin. Tumor volume was calculated as $L \times W^2 \times \pi/6$ and recorded twice per week. All animals were housed in pathogen-free facilities and provided with abundant food and water under guidelines approved by the MSKCC Institutional Animal Care and Use Committee and Research Animal Resource Center.

33. M. E. Arcila, G. R. Oxnard, K. Nafa, G. J. Riely, S. B. Solomon, M. F. Zakowski, M. G. Kris, W. Pao, V. A. Miller, M. Ladanyi, Rebiopsy of lung cancer patients with acquired resistance to EGFR inhibitors and enhanced detection of the T790M mutation using a locked nucleic acid-based assay. *Clin. Cancer Res.* **17**, 1169–1180 (2011).
34. D. T. Milton, C. G. Azzoli, R. T. Heelan, E. Venkatraman, J. E. Gomez, M. G. Kris, L. M. Krug, W. Pao, N. A. Rizvi, M. Dunne, V. A. Miller, A phase III study of weekly high-dose erlotinib in previously treated patients with nonsmall cell lung cancer. *Cancer* **107**, 1034–1041 (2006).
35. M. Hidalgo, L. L. Siu, J. Nemunaitis, J. Rizzo, L. A. Hammond, C. Takimoto, S. G. Eckhardt, A. Tolcher, C. D. Britten, L. Denis, K. Ferrante, D. D. Von Hoff, S. Silberman, E. K. Rowinsky, Phase I and pharmacologic study of OSI-774, an epidermal growth factor receptor tyrosine kinase inhibitor, in patients with advanced solid malignancies. *J. Clin. Oncol.* **19**, 3267–3279 (2001).
36. E. Parzen, *Stochastic Processes* (Society for Industrial and Applied Mathematics, Philadelphia, PA, 1999).
37. F. C. Detterbeck, C. J. Gibson, Turning gray: The natural history of lung cancer over time. *J. Thorac. Oncol.* **3**, 781–792 (2008).
38. R. Seshadri, R. J. Kutlaca, K. Trainor, C. Matthews, A. A. Morley, Mutation rate of normal and malignant human lymphocytes. *Cancer Res.* **47**, 407–409 (1987).
39. A. R. Oller, P. Rastogi, S. Morgenthaler, W. G. Thilly, A statistical model to estimate variance in long term-low dose mutation assays: Testing of the model in a human lymphoblastoid mutation assay. *Mutat. Res.* **216**, 149–161 (1989).
40. F. A. Eskens, C. H. Mom, A. S. Planting, J. A. Gietema, A. Amelsberg, H. Huisman, L. van Doorn, H. Burger, P. Stopfer, J. Verweij, E. G. de Vries, A phase I dose escalation study of BIBW 2992, an irreversible dual inhibitor of epidermal growth factor receptor 1 (EGFR) and 2 (HER2) tyrosine kinase in a 2-week on, 2-week off schedule in patients with advanced solid tumours. *Br. J. Cancer* **98**, 80–85 (2008).
41. R. J. Gralla, E. S. Casper, D. P. Kelsen, D. W. Braun Jr., M. E. Dukeman, N. Martini, C. W. Young, R. B. Golbey, Cisplatin and vindesine combination chemotherapy for advanced carcinoma of the lung: A randomized trial investigating two dosage schedules. *Ann. Intern. Med.* **95**, 414–420 (1981).
42. L. M. Krug, K. K. Ng, M. G. Kris, V. A. Miller, W. Tong, R. T. Heelan, L. Leon, D. Leung, J. Kelly, S. C. Grant, F. M. Sirotnak, Phase I and pharmacokinetic study of 10-propargyl-10-deazaaminopterin, a new antifolate. *Clin. Cancer Res.* **6**, 3493–3498 (2000).
43. C. G. Azzoli, L. M. Krug, J. Gomez, V. A. Miller, M. G. Kris, M. S. Ginsberg, R. Henry, J. Jones, L. Tyson, M. Dunne, B. Pizzo, A. Farmer, E. Venkatraman, R. Steffen, F. M. Sirotnak, A phase 1 study of pralatrexate in combination with paclitaxel or docetaxel in patients with advanced solid tumors. *Clin. Cancer Res.* **13**, 2692–2698 (2007).
44. W. L. Yeo, G. J. Riely, B. Y. Yeap, M. W. Lau, J. L. Warner, K. Bodio, M. S. Huberman, M. G. Kris, D. G. Tenen, W. Pao, S. Kobayashi, D. B. Costa, Erlotinib at a dose of 25 mg daily for non-small cell lung cancers with EGFR mutations. *J. Thorac. Oncol.* **5**, 1048–1053 (2010).
45. K. L. Blackwell, H. J. Burstein, A. M. Storniolo, H. Rugo, G. Sledge, M. Koehler, C. Ellis, M. Casey, S. Vukelja, J. Bischoff, J. Baselga, J. O'Shaughnessy, Randomized study of lapatinib alone or in combination with trastuzumab in women with ErbB2-positive, trastuzumab-refractory metastatic breast cancer. *J. Clin. Oncol.* **28**, 1124–1130 (2010).
46. N. Godin-Heymann, I. Bryant, M. N. Rivera, L. Ulkus, D. W. Bell, D. J. Riese II, J. Settleman, D. A. Haber, Oncogenic activity of epidermal growth factor receptor kinase mutant alleles is enhanced by the T790M drug resistance mutation. *Cancer Res.* **67**, 7319–7326 (2007).
47. T. G. Bivona, H. Hieronymus, J. Parker, K. Chang, M. Taron, R. Rosell, P. Moonsamy, K. Dahlman, V. A. Miller, C. Costa, G. Hannon, C. L. Sawyers, FAS and NF- κ B signalling modulate dependence of lung cancers on mutant EGFR. *Nature* **471**, 523–526 (2011).
48. Y. Gong, E. Yao, R. Shen, A. Goel, M. Arcila, J. Teruya-Feldstein, M. F. Zakowski, S. Frankel, M. Peifer, R. K. Thomas, M. Ladanyi, W. Pao, High expression levels of total IGF-1R and sensitivity of NSCLC cells in vitro to an anti-HGF-1R antibody (R1507). *PLoS One* **4**, e7273 (2009).
49. K. E. Ware, M. E. Marshall, L. R. Heasley, L. Marek, T. K. Hinz, P. Hercule, B. A. Helfrich, R. C. Doebele, L. E. Heasley, Rapidly acquired resistance to EGFR tyrosine kinase inhibitors in NSCLC cell lines through de-repression of FGFR2 and FGFR3 expression. *PLoS One* **5**, e14117 (2010).
50. A. D. Van den Abbeele, R. D. Badawi, J. Manola, J. A. Morgan, J. Desai, A. Kazanovicz, M. St. Armand, C. Baum, G. D. Demetri, Effects of cessation of imatinib mesylate (IM) therapy in patients (pts) with IM-refractory gastrointestinal stromal tumors (GIST) as visualized by FDG-PET scanning. *J. Clin. Oncol.* **22**, 3012 (2004).
51. E. Fumagalli, P. Coco, C. Morosi, P. Dileo, R. Bertulli, A. Gronchi, P. G. Casali, Rechallenge with imatinib in GIST patients resistant to second or third line therapy, abstract presented at the 15th Connective Tissue Oncology Society Meeting, Miami Beach, FL, 2009.
52. B. Hanfstein, M. C. Müller, S. Kreil, T. Ernst, T. Schenk, C. Lorentz, U. Schwindel, A. Leitner, R. Hehlmann, A. Hochhaus, Dynamics of mutant BCR-ABL-positive clones after cessation of tyrosine kinase inhibitor therapy. *Haematologica* **96**, 360–366 (2011).
53. P. Therasse, S. G. Arbuck, E. A. Eisenhauer, J. Wanders, R. S. Kaplan, L. Rubinstein, J. Verweij, M. Van Glabbeke, A. T. van Oosterom, M. C. Christian, S. G. Gwyther, New guidelines to evaluate the response to treatment in solid tumors. European Organization for Research and Treatment of Cancer, National Cancer Institute of the United States, National Cancer Institute of Canada. *J. Natl. Cancer Inst.* **92**, 205–216 (2000).
54. Y. Iwasa, M. A. Nowak, F. Michor, Evolution of resistance during clonal expansion. *Genetics* **172**, 2557–2566 (2006).
55. J. Foo, F. Michor, Evolution of resistance to anti-cancer therapy during general dosing schedules. *J. Theor. Biol.* **263**, 179–188 (2010).
56. **Acknowledgments:** We thank Y. Lin for assistance with PCRs, R. Maki for helpful discussions, and C. Arteaga and G. Riely for critically reviewing the manuscript. **Funding:** Supported by NIH/National Cancer Institute (NCI) grants R01-CA121210 (W.P.), P01-CA129243 (M.G.K. and W.P.), and U54-CA143798 (F.M. and W.P.). The MSKCC Genomics Core is supported by an NCI Cancer Center Support Grant award to MSKCC (P30-CA008748). W.P. received additional support from Vanderbilt's SPORE in Lung Cancer grant (CA90949) and the Vanderbilt-Ingram Cancer Center Core grant (P30-CA68485). R.K.T. is supported by the German Ministry of Science and Education as part of the NGFNplus program (grant 01GS08100), Max Planck Society (MLFANEUR8061), Deutsche Forschungsgemeinschaft through SFB832 (TP6), Deutsche Krebshilfe (grant 107954), and Fritz-Thyssen-Stiftung (grant 10.082.175). **Author contributions:** J.C. and W.P. conceived the project and wrote the initial draft of the manuscript. J.C., J.F., K.H., K.O., R.S., L.W., K.R.A., M.L.S., and E.D.S. performed the experiments. J.C., J.F., G.R.O., M.A., N.D.S., A.V., M.S.G., M.G.K., M.L., V.A.M., F.M., and W.P. analyzed the data. A.I. contributed unpublished patient data sets. All authors commented on the final version of the manuscript. **Competing interests:** R.K.T. has received consulting and lecture fees from Sequenom, Sanofi-Aventis, Merck, Roche, Infinity, Boehringer-Ingelheim, AstraZeneca, Johnson & Johnson, and Atlas-Biolabs, and research support from Novartis and AstraZeneca. V.A.M. has consulted for Boehringer-Ingelheim, Genentech, and Roche. M.G.K. has consulted for Boehringer-Ingelheim and Allos Therapeutics. A.I. has consulted for AstraZeneca and Chugai. W.P. has consulted for MolecularMD and AstraZeneca. Rights to a patent application for EGFR T790M testing were licensed on behalf of V.A.M., W.P., and others to MolecularMD. The patent application has been filed by MSKCC.

Submitted 7 March 2011

Accepted 13 May 2011

Published 6 July 2011

10.1126/scitranslmed.3002356

Citation: J. Chmielecki, J. Foo, G. R. Oxnard, K. Hutchinson, K. Ohashi, R. Somwar, L. Wang, K. R. Amato, M. Arcila, M. L. Sos, N. D. Socci, A. Viale, E. de Stanchina, M. S. Ginsberg, R. K. Thomas, M. G. Kris, A. Inoue, M. Ladanyi, V. A. Miller, F. Michor, W. Pao, Optimization of dosing for EGFR-mutant non-small cell lung cancer with evolutionary cancer modeling. *Sci. Transl. Med.* **3**, 90ra59 (2011).

Supplementary Materials for
**Optimization of Dosing for EGFR-Mutant Non-Small Cell Lung
Cancer with Evolutionary Cancer Modeling**

Juliann Chmielecki, Jasmine Foo, Geoffrey R. Oxnard, Katherine Hutchinson, Kadoaki Ohashi, Romel Somwar, Lu Wang, Katherine R. Amato, Maria Arcila, Martin L. Sos, Nicholas D. Socci, Agnes Viale, Elisa de Stanchina, Michelle S. Ginsberg, Roman K. Thomas, Mark G. Kris, Akira Inoue, Marc Ladanyi, Vincent A. Miller, Franziska Michor,* William Pao*

*To whom correspondence should be addressed. E-mail: michor@jimmy.harvard.edu (F.M.); william.pao@vanderbilt.edu (W.P.)

Published 6 July 2011, *Sci. Transl. Med.* 3, 90ra59 (2011)
DOI: 10.1126/scitranslmed.3002356

The PDF file includes:

Materials and Methods

Fig. S1. Further characterization of PC-9 TKI-resistant cell lines.

Fig. S2. Characterization of *EGFR*-mutant TKI-resistant cells.

Fig. S3. Characterization of H3255 TKI-resistant cells.

Fig. S4. Rate of progression in T790M-harboring *EGFR*-mutant lung cancer.

Fig. S5. Derivation of mathematical parameters.

Fig. S6. Continuation of TKI therapy in cell populations with T790M-harboring clones leads to better tumor cell control.

Fig. S7. Toxicity of “gatekeeper” mutations in other cell models.

References

SUPPLEMENTARY MATERIALS AND METHODS

***EGFR* sequencing**

Genomic DNA was extracted from patient samples ($\geq 70\%$ tumor cells) and cell lines using standard procedures. Dideoxynucleotide sequencing of *EGFR* (exons 2-28) was performed as described (S1).

For 454 deep sequencing of *EGFR* exon 20, 80 ng of genomic DNA per sample was used for PCR amplification with 454 barcoded primers (F1: GCCTCCCTCGCGCCATCAGACGAGTGCGTACACTGACGTGCCCTCTCCCT or F2:GCCTCCCTCGCGCCATCAGACGCTCGACAACACTGACGTGCCCTCTCCCT and R: GCCTTGCCAGCCCGCTCAGCGTATCTCCCTTCCCTGATT). PCR was performed with *Pfu* polymerase to ensure greater sequence accuracy. PCR products were separated from excess primers and dNTPs using AMPure reagent (Agencourt), as per the manufacturer's instructions. Approximately 100,000 reads per sample were generated using a 454 FLX platform (Roche). Alignment and variant detection was carried out using the ssahaSNP algorithm from the Sanger Institute (S2). The output of the ssahaSNP pipeline was then filtered by a set of custom written python scripts to filter on various quality metrics including total coverage, variant coverage, integrated and average Q score and frequency of variant.

Cell culture and derivation of TKI-resistant lines

EGFR mutant PC-9 cells (del E746-A750) (S3) or HCC827 cells (del E746-A750) were cultured in RPMI media (ATCC or Mediatech) supplemented with 10% heat

inactivated fetal bovine serum (Gemini Bio Products) and pen-strep solution (Gemini Bio Products; final concentration 100U/mL penicillin, 100µg/mL streptomycin). Cells were grown in a humidified incubator with 5% CO₂ at 37°C. Resistant cells were derived as described (S4, S5). NR-6 and H322M cells have been previously reported (S6, S7).

To create EGFR TKI resistant lines, parental cells were cultured with increasing concentrations of TKIs starting with the IC₃₀. Doses were increased in a stepwise pattern when normal cell proliferation patterns resumed. Fresh drug was added every 72-96 hours. Resistant cells that grew in 500 nM BIBW-2992 and 5 µM erlotinib were derived after ~ 3 months of culturing with drug. Resistant cells were maintained initially as polyclonal populations under constant TKI selection. Clonal resistant cells were isolated by limiting dilution.

aCGH profiling

Genomic DNA from cell lines and controls was prepared, labeled, and hybridized to Agilent 244k arrays, as previously described (S8). Analysis was performed using DNA Analytics software (Agilent).

Immunoblotting

Cells were washed with cold PBS and lysed for 30 minutes with RIPA buffer (150mM Tris.HCl pH 7.5, 150mM NaCl, 1% NP-40 substitute, 0.1% SDS) supplemented with protease inhibitor cocktail (Roche), 40mM sodium fluoride, 1mM sodium orthovanadate, and 1µM okadaic acid. Protein was quantified with Bradford Reagent

(Bio-Rad) and equal amounts were loaded for SDS-PAGE with 4-20% acrylamide pre-cast gels (Invitrogen), followed by transfer to PVDF membranes. Membranes were blotted with pEGFR (Y1068/1092), total EGFR (BD Biosciences), pAKT (S473), total AKT, pERK (T202/204), total ERK, and actin (Sigma-Aldrich) followed by HRP-conjugated secondary antibodies. All antibodies were purchased from Cell Signaling Technology, unless noted. Signals were detected with Western blotting detection reagents (GE Healthcare).

Thymidine Incorporation

Thymidine incorporation was determined as described previously with some modifications (S9). Briefly, cells were seeded at a density of 20,000 cells per well in 24-well tissue culture plates and incubated with compounds for 24 hours. ³H-methyl thymidine (1 μ Ci/mL) was added during the last 2 hours of drug treatment. Cells were then washed three times with ice-cold 10% TCA (v/v) and then lysed in 500 μ L 0.5 M NaOH (v/v) per well. The amount of labeled thymidine incorporated into DNA was determined by liquid scintillation counting. Protein concentration was determined in parallel samples and results were corrected for protein expression.

Fluorescence in situ hybridization (FISH)

Cells were grown in RPMI 1640 with 10% FBS to ~70% confluence. One hour prior to harvest, colcemid (Invitrogen) was added into each flask containing 10 mL growth medium. Metaphase FISH slides preparation was performed as previously described (S8).

The EGFR/CEP7 probe set from Abbott Molecular was used for dual-color FISH. FISH was performed according to the protocol from Vysis/Abbott Molecular with a few modifications. In brief, a probe targeting the EGFR gene was labeled with SpectrumOrange (red), and a Chromosome 7 centromere probe (CEP7) was labeled with SpectrumGreen (green); nuclei were counterstained with DAPI (blue). FISH slide analysis and signal capture were performed by Fluorescence microscope (Zeiss) coupled with ISIS FISH Imaging System (Metasystems) following the manufacturer's instruction. Metaphases showing optimum hybridization signals were scored. 6 representative metaphases of each sample were captured.

Drug Sources

Cisplatin was obtained from the VICC and MSKCC pharmacies. Pralatrexate was also obtained from the MSKCC pharmacy. Erlotinib and BIBW-2992 were synthesized at the MSKCC organic synthesis core.

Figure S1

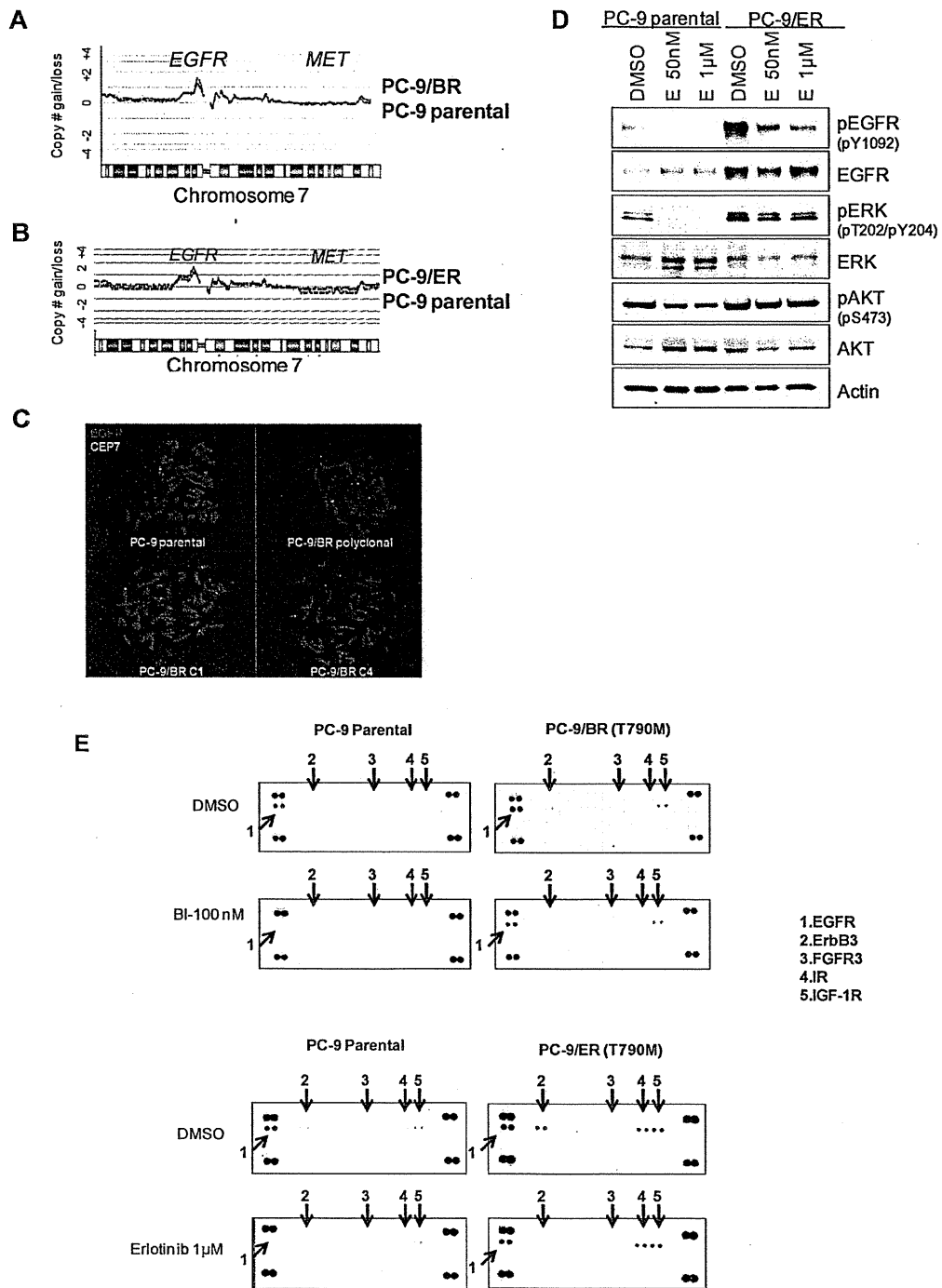


Figure S1. Further characterization of PC-9 TKI-resistant cell lines. (A) Array comparative genomic hybridization (aCGH) of chromosome 7 shows further amplification of *EGFR* in the BIBW-2992-resistant cells (PC-9/BR; red) and the erlotinib-resistant cells (PC-9/ER) (B) versus the parental cells (blue). Neither cell line, however, displayed amplification of *MET*, another receptor tyrosine kinase involved in TKI-resistance. The relative positions of *EGFR* and *MET* are labeled on the chromosome. (C) Fluorescence in situ hybridization (FISH) staining of metaphase cells confirms the genomic amplification of *EGFR* in the BR polyclonal cells and two resistant clones compared to parental cells. *EGFR* was not amplified on double minute chromosomes, a previously reported mechanism of resistance and TKI re-sensitization. *EGFR* is labeled in red; chromosome 7 centromere (CEP7) is labeled in green. (D) Parental and resistant (ER) cells were treated with vehicle (DMSO) or erlotinib (E) for 3 hours prior to protein isolation. Parental cells show decreased phosphorylation of EGFR and its downstream targets, ERK and AKT, in the presence of low (50 nM) and high (1 μ M) concentrations of erlotinib. Signaling in the PC-9/ER cells remains intact, regardless of the concentration of drug. (E) Phospho-receptor tyrosine kinase (RTK) arrays profiling PC-9 parental, ER, and BR cells in the presence and absence of TKI do not show any dramatic differences between the T790M-harboring lines derived with two different TKIs.

Figure S2

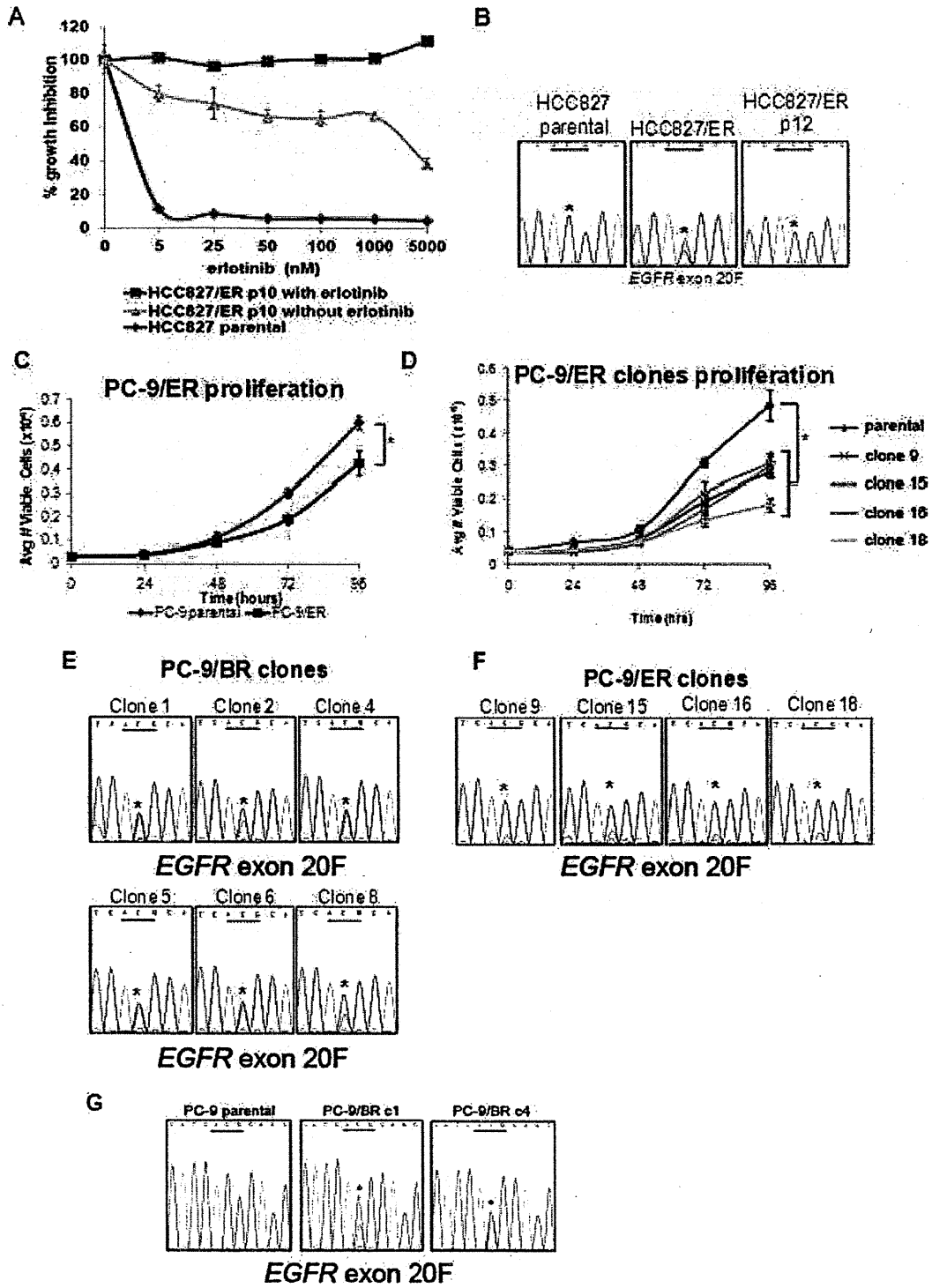


Figure S2. Characterization of EGFR-mutant TKI-resistant cells. (A) Polyclonal HCC827/ER cells, harboring *EGFR* T790M, were derived after ~150 days in culture with increasing concentrations of erlotinib. Once resistant, cells were then maintained in erlotinib or drug was removed from the culture. Following 10 passages without drug (P12), the cells regained intermediate sensitivity to erlotinib, as shown in growth inhibition assays. By contrast, cells passaged in parallel with erlotinib for 10 passages remained resistant. (B) Direct sequencing chromatograms from *EGFR* exon 20 show the presence of T790M (starred) in the HCC827/ER cells and a decrease of the mutant allele in DNA from cells that had been passaged 12 times in the absence of erlotinib (p-12). (C) The T790M-containing PC-9/ER cells proliferate more slowly than their parental counterparts. PC-9 parental and ER cells were counted in triplicate over 72 hours in the absence of inhibitor, and the average number of viable cells was plotted +/- standard deviation. (D) PC-9/ER clonal cells (derived from polyclonal PC-9/ER cells) also proliferate more slowly than the parental cells. Cells were counted and plotted as described above. (* $p < 0.01$). (E) Direct sequencing chromatograms from *EGFR* exon 20 show all BR clones contain the T790M mutation (starred). (F) T790M is also observed in clones derived from PC-9/ER cells, at slightly lower levels. (G) Direct sequencing chromatograms from *EGFR* exon 20 with DNA extracted from PC-9 parental, PC-9/BR c1, and PC-9/BR c4 xenograft tumors (see **Figure 2G**). The presence of the mutant T790M is starred in c1 and c4. Note that mice with parental tumors had to be sacrificed after 34 days post implantation due to tumor size, while mice with c1 and c4 tumors were not sacrificed until 78 days post implantation.

Figure S3

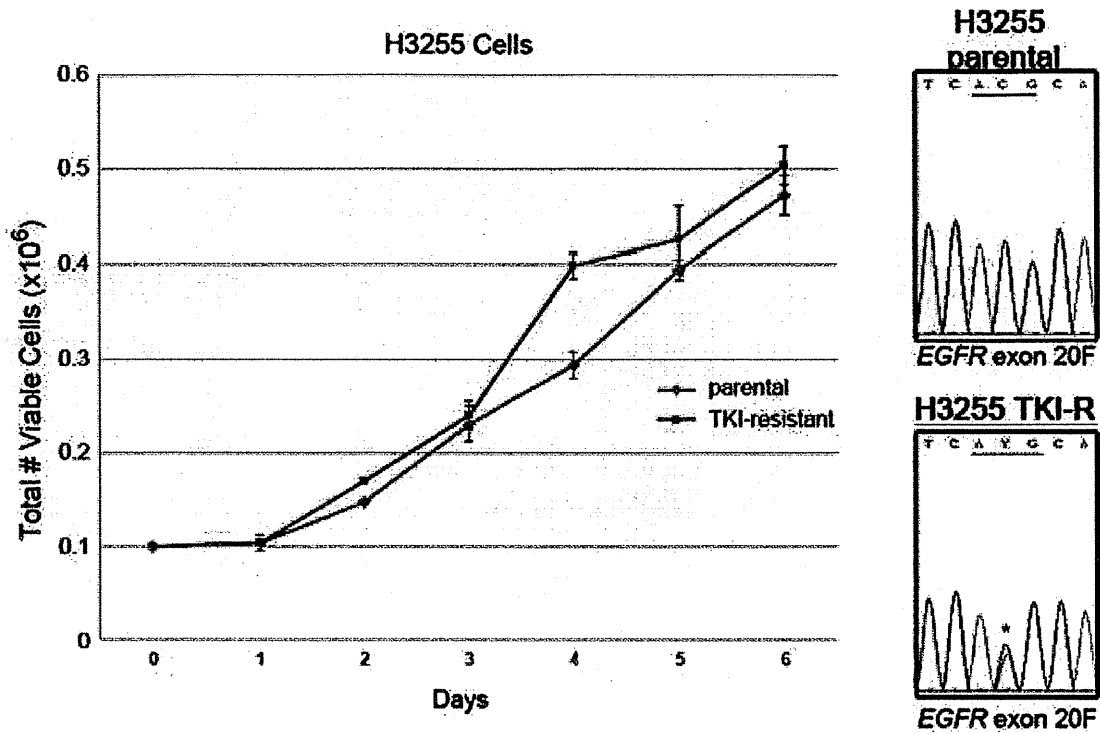


Figure S3. Characterization of H3255 TKI-resistant cells. H3255 parental and TKI-resistant cells were counted daily in the absence of drug. The TKI-resistant cells harbor the T790M-mutation, as shown by direct sequencing of EGFR exon 20 (right panel). Unlike the PC-9 cells, the H3255 TKI-R did not exhibit a growth disadvantage compared to their parental counterparts.

Figure S4

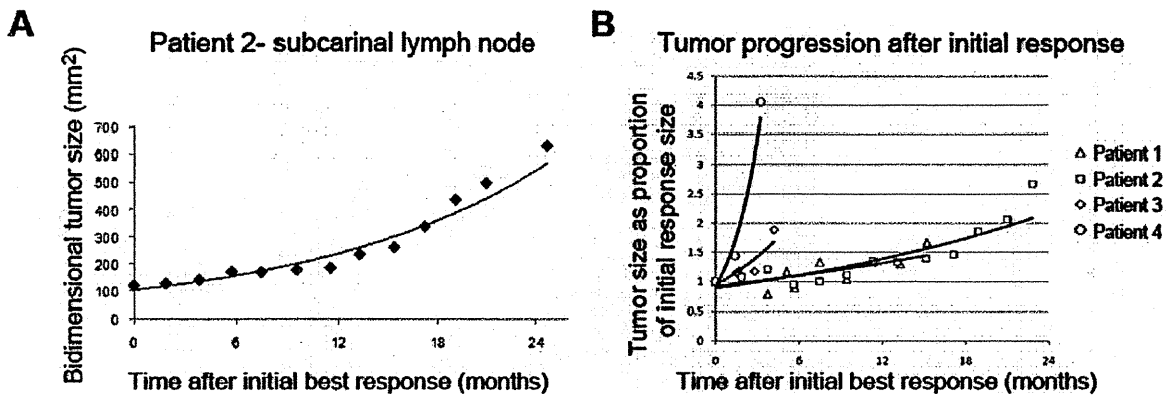


Figure S4. Rate of progression in T790M-harboring *EGFR*-mutant lung cancer.

(A) Bi-dimensional measurements from a second patient with *EGFR* mutant lung cancer show an indolent rate of progression following progressive disease (as determined by RECIST criteria; see **Methods**). (B) As a comparison, we reviewed the imaging of disease in patients with *EGFR* wild-type tumors who responded to first-line platinum based chemotherapy on a separate prospective clinical trial. Patients 1 and 2 are the same as those shown in **Figures 4C and S4A**, respectively. T790M-harboring tumors (patients 1 and 2) displayed a slow increase in tumor size, eventually meeting criteria for progressive disease. However, *EGFR* wildtype tumors (patients 3 and 4) had a rapid increase in tumor size between the scan showing progressive disease and the previous scan.